

STUDYING NF-KAPPA B TRANSLOCATION BETWEEN NUCLEUS AND CYTOPLASM BY ELECTROPORATIVE FLOW CYTOMETRY

Jun Wang¹, Bei Fei², Yihong Zhan³, Robert L. Geahlen² & Chang Lu³

¹*Birck Nanotechnology Center, ²Department of Medicinal Chemistry and Molecular Pharmacology, Purdue University, West Lafayette, Indiana 47907, USA.*

³*Department of Chemical Engineering, Virginia Tech, Blacksburg, Virginia 24061, USA.*

ABSTRACT

Transport of protein and RNA cargoes between the nucleus and cytoplasm (nucleocytoplasmic transport) is vital for a variety of cellular functions. In this report, we describe using a novel method, microfluidic electroporative flow cytometry, to study kinetics of nucleocytoplasmic transport of an important transcription factor NF- κ B. With data collected from single cells, we quantitatively characterize the population-averaged kinetic parameters such as the rate constants and apparent activation barrier for NF- κ B transport. Our data demonstrate that NF- κ B nucleocytoplasmic transport fits first-order kinetics very well and is a fairly reversible process governed by equilibrium thermodynamics.

Keywords: Electroporative flow cytometry, NF- κ B, Microfluidic, Translocation, Nucleocytoplasmic transport

INTRODUCTION

A eukaryotic cell is divided by the nuclear membrane into two compartments with efficient and selective interchange of proteins, nucleic acids, and small molecules. Transport of protein and RNA cargoes between the nucleus and cytoplasm has been recognized as a critical process for the molecules to carry out their cellular functions [1-3]. Nucleocytoplasmic transport is often regulated via upstream signal transduction pathways that lead to protein modifications or the masking or unmasking of the nuclear transport signals. As expected, alterations in any of the regulatory steps can result in the mislocalization of a protein leading to various disease states ranging to metabolic disorders to cancer [4]. Not surprisingly, modification of the nucleocytoplasmic transport of specific target molecules has been proposed and practiced as an interesting therapeutic approach for disease treatment [4].

In this study, we use a single-cell technique that combines electroporation with flow cytometry, referred to as Electroporative Flow Cytometry (EFC)[5], for obtaining quantitative information on the kinetics of nucleocytoplasmic transport. Our approach does not require obtaining images of cells and therefore permits the use of a single element detector (e.g. a photomultiplier tube), which is essential for high throughput and easy quantification. Taking advantage of the fact that the release of an intracellular protein due to electroporation is dependent on the protein's subcellular location, we quantify the cytosolic and nuclear fractions of a transcription factor NF- κ B at the single cell level for a cell population during its nucleocytoplasmic transport. The data allow us to calculate the rate constants and the apparent activation barrier by fitting the process with first-order kinetics. The results indicate that the nucleocytoplasmic transport of NF- κ B is governed by equilibrium thermodynamics and the transport process is more reversible than the prototypical nuclear import of proteins with NLS.

EXPERIMENTAL

Microchip fabrication. Microfluidic electroporative flow cytometry (EFC) devices were fabricated based on PDMS using the standard soft lithography method described previously [6].

Cell sample preparation. CHO/GFP-NF κ Bp65 cell line (Panomics) was created by co-transfection of an expression vector for a fusion protein of turboGFP (Evrogen) and human NF κ Bp65, as well as pHyg into Chinese hamster ovary (CHO) cells. CHO cells were subcultured for every 2 days in Hams F12K media supplemented with 10% fetal bovine serum, 100 IU/ml penicillin G, 100 μ g/ml streptomycin and 100 μ g/ml hygromycin. The harvested cells were either cultured in petri dishes or 96 well plates for 24 hr before starvation for 4 hr in serum free media. To stimulate adherent cells, the complete Hams F12K media supplemented with IL-1 β at 20 ng/ml was used to replace starvation medium. Cells were detached by addition of 0.25% trypsin-EDTA for 1 min and washed twice by an electroporation buffer (1 mM MgSO₄, 8 mM Na₂HPO₄, 2 mM KH₂PO₄, and 250 mM sucrose, pH 7.2). To stimulate cells in suspension, cells (1 \times 10⁶/ml) were suspended in the electroporation buffer with 20 ng/ml IL-1 β and incubated at the indicated temperature for the designated periods of time. All cell samples were centrifuged at 300 \times g for 10 min and resuspended in the electroporation buffer at a final density of 1 \times 10⁷ cells/ml before a microfluidic EFC experiment.

Microchip operation and cytometry detection. The microfluidic chip was mounted on the microscope. The 3 inlets of the channel were connected to a syringe pump (PHD infusion pump, Harvard Apparatus) through plastic tubing. A high voltage power supply (PS350, Stanford Research Systems) was used to generate a constant direct current (DC) voltage between the electrodes. A 488 nm laser beam (air-cooled 100 mW argon ion laser, Spectra-Physics) was focused in the microfluidic channel at 150 μ m downstream of the intersection (**Fig. 1a**). The emission light by laser excitation was collected by the same objective and converted into current which was then converted to voltage and input into a PCI data acquisition card (PCI-6254, National Instruments) operated by LabView software (National Instruments). The data were processed by programs written in MATLAB to extract histograms of the fluorescence for a cell population. The voltage

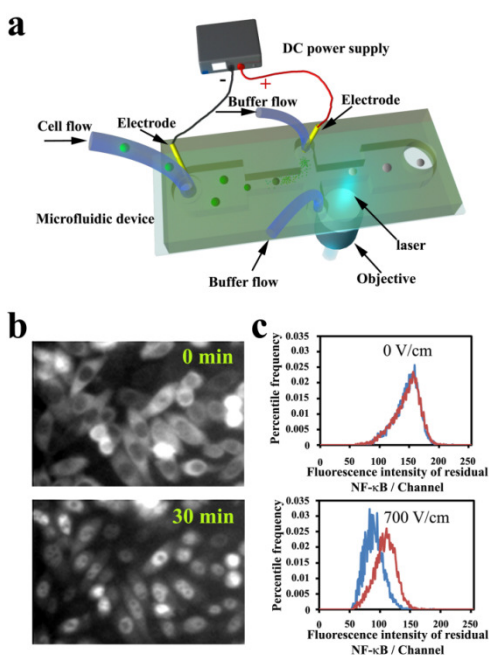


Fig. 1 (a) Schematic of the microfluidic electroporative flow cytometry device. The microfluidic device is mounted on a microscope that allows incident laser from a 40X objective to focus in the channel. A DC power supply generates a constant high electric field in the narrow sections to electroporate cells and release intracellular proteins. (b) Fluorescence images of CHO cells expressing GFP labeled NF- κ B. The cells were stimulated by 20 ng/ml IL-1 β at 37 $^{\circ}$ C at time 0. (c) Comparison of histograms of residual NF- κ B between stimulated cells (red) and cells without stimulation (blue) under electric fields of 0 and 700 V/cm. The electroporation duration was 120 ms. The stimulation was conducted at 37 $^{\circ}$ C for 30 min.

signal ranging from 1 mV to 1 V was converted to 4 decade logarithmic voltage scale and then 256 scale channels, due to the relative small sample size of 6000-10000 cells in each histogram. The fluorescence signal was also converted into MESF units.

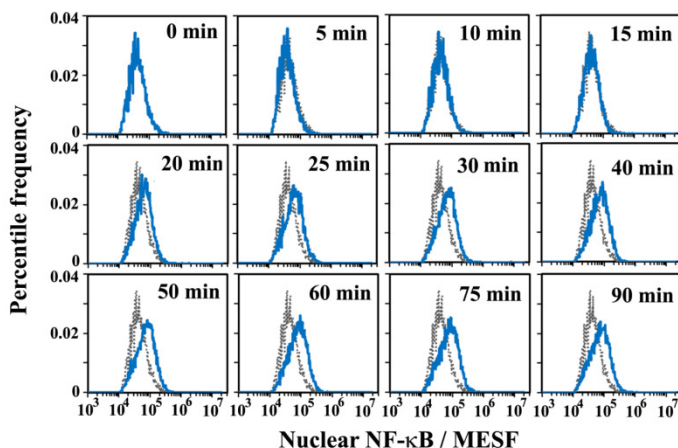
RESULTS AND DISCUSSION

As shown in **Fig. 1a**, cells were allowed to flow through a microfluidic channel with a narrow middle section under hydrodynamic focusing. A constant voltage was established across two

reservoirs of the microfluidic channels such that only the field intensity in the narrow section was high enough to produce electroporation [6]. The nanoscale pores generated in the plasma membrane of cells by electroporation allowed intracellular molecules to be released into the surrounding solution [7-12]. In this system, the released proteins (including GFP labeled NF- κ B) moved into the upper reservoir under the influence of the electric field without interfering with the laser-induced fluorescence detection while the remaining single cells (after release) flowed to the downstream laser detection point and generated signals that were collected by a photomultiplier tube (PMT).

We found that the cytosolic fraction of a protein was released more readily during electroporation than the nuclear fraction of the same protein, presumably due to lack of an enclosure provided by the nuclear envelope and closer proximity to the plasma membrane. As shown in **Fig. 1b**, when NF- κ B was activated (induced by IL-1 β), a substantial portion moved into the nucleus. Consistent with this, the stimulated cell population retained a significantly larger amount of residual NF- κ B after electroporation than did the unstimulated population. Such a difference could readily be observed from the histograms generated by the two populations (**Fig. 1c**, lower panel) and fluorescence images. In comparison, when there was no electric field, the device worked similarly to a conventional flow cytometer and no difference between the populations was detected (**Fig. 1c**, upper panel). Such a relationship between the electroporation-based release and the subcellular localization of the protein serves as the basis for our detection of nucleocytoplasmic transport without imaging.

By quantifying the release of two marker intracellular proteins (p38, which is located in the cytosol and Sp1, which is nuclear) [13] by electroporation using Western blot analysis, we also estimated that, with an electroporation field intensity >600 V/cm and duration >100 ms, 100% of cytosolic proteins and 27% of nuclear proteins were released into the solution. It is worth noting that this estimation omits the effects of the type and amount of a protein on its release. Using these estimations and EFC data taken under the optimized operating conditions (120 ms and 700 V/cm), we were able to calculate the amount of NF- κ B that was originally in the nucleus based on the residual NF- κ B amount after electroporation at the single cell level (In this case the original amount was roughly a factor of 1.37 more than the residual amount, if we ignored the difference in the release pattern among cells).



The fluorescence signal detected by the PMT was converted into Molecules of Equivalent Soluble Fluorophores (MESF) units for quantification purpose. **Fig. 2** shows quantitatively that the histograms of nuclear NF- κ B amount (in MESF) shifted toward the higher end over time after stimulation by IL-1 β at 30 $^{\circ}$ C, indicating the

Fig. 2 The histograms of nuclear NF- κ B amount (in MESF) at different times after stimulation. The grey histogram was taken at time 0 and serves as a reference for the other histograms taken at later time points. The electroporative flow cytometry was conducted with an electroporation field of 700 V/cm and a duration of 120 ms. The cells were stimulated by 20 ng/ml IL-1 β at 30 $^{\circ}$ C.

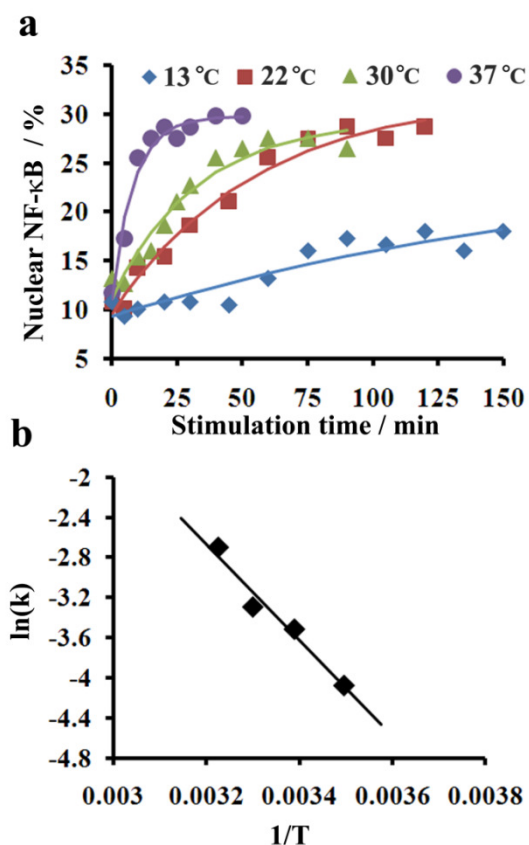


Fig. 3 Kinetics of NF-κB nucleocytoplasmic transport. (a) Effect of temperature on nucleocytoplasmic transport rate. The data points are experimental data and the curves are fitted assuming first-order kinetics. (b) Arrhenius plot for calculating the apparent activation barrier E_a . E_a is calculated based on Arrhenius equation $\ln(k) = -\frac{E_a}{RT} + C$ where k is the rate constant, R is the gas constant and C is a constant.

ACKNOWLEDGEMENTS

We thank NSF CBET 1016547 and NIH NCI CA115465 for financial support of this research.

REFERENCES

- [1] E.A. Nigg, Nature, 386 (1997) 779.
- [2] S. Nakielny and G. Dreyfuss, Cell, 99 (1999) 677.
- [3] L.J. Terry, E.B. Shows and S.R. Wentz, Science, 318 (2007) 1412.
- [4] T.R. Kau, J.C. Way and P.A. Silver, Nat Rev Cancer, 4 (2004) 106.
- [5] J. Wang, N. Bao, L.L. Paris, H.Y. Wang, R.L. Geahlen and C. Lu, Analytical Chemistry, 80 (2008) 1087.
- [6] H.Y. Wang and C. Lu, Analytical Chemistry, 78 (2006) 5158.
- [7] F. Ryttsen, C. Farre, C. Brennan, S.G. Weber, K. Nolkrantz, K. Jardemark, D.T. Chiu and O. Orwar, Biophysical Journal, 79 (2000) 1993.
- [8] M.A. McClain, C.T. Culbertson, S.C. Jacobson, N.L. Allbritton, C.E. Sims and J.M. Ramsey, Analytical Chemistry, 75 (2003) 5646.
- [9] H. Lu, M.A. Schmidt and K.F. Jensen, Lab Chip, 5 (2005) 23.
- [10] P.J. Marc, C.E. Sims, M. Bachman, G.P. Li and N.L. Allbritton, Lab Chip, 8 (2008) 710.
- [11] A. Valero, J.N. Post, J.W. van Nieuwkastele, P.M. Ter Braak, W. Kruijer and A. van den Berg, Lab Chip, 8 (2008) 62.
- [12] A. Agarwal, M.Y. Wang, J. Olofsson, O. Orwar and S.G. Weber, Analytical Chemistry, 81 (2009) 8001.
- [13] F. Zhou, J. Hu, H. Ma, M.L. Harrison and R.L. Geahlen, Mol Cell Biol, 26 (2006) 3478.

gradual transport of NF-κB into the nucleus. These histograms present details about the cell populations during the transport event with single cell resolution.

Taking advantage of the quantitative nature of our cytometry data, we were able to quantify the kinetics and activation barrier of the nucleocytoplasmic transport of NF-κB. The histograms such as those taken in Fig. 2 allow us to follow the progress of nucleocytoplasmic transport at the population level. We were able to generate plots indicating the change in the percent of nuclear NF-κB for the population over time at different stimulation temperatures between 13 and 37 °C (Fig. 3a). In general, the transport occurred faster when the temperature was higher (Fig. 3a), consistent with what was revealed by Western blot analysis. The time course data in Fig. 3a fit very well ($R^2 \sim 0.94$) with a first-order process

$$N = N_{ss} + (N_0 - N_{ss})e^{-kt} \quad [\text{Eqn. 1}]$$

where N is the percent of nuclear NF-κB, N_{ss} is the steady state value of the percent of nuclear NF-κB (the endpoint of the nucleocytoplasmic transport), N_0 is the initial percent of nuclear NF-κB at time 0, and k is the first-order rate constant. The fitting of these curves generated values for k , N_0 , and N_{ss} at various temperatures. The percentage of nuclear NF-κB at the beginning of the translocation ($N_0 = 10.3 \pm 1.0\%$) and that at the end of the translocation ($N_{ss} = 29.2 \pm 2.3\%$) appear to be fairly consistent under different temperatures. In Fig. 3b, the Arrhenius plot generates an apparent activation barrier of 39.8 KJ/mol for the temperature range of 13-37 °C.

CONCLUSIONS

Our approach generates highly quantitative kinetics data on the protein transport at the ensemble level by putting together information collected from single cells. These data provide the basis to compare the effectiveness of the machinery required for different molecules undergoing nucleocytoplasmic transport and to assess how these processes are affected by agents such as anticancer drugs. Such information is critical for understanding the hierarchical regulation of protein translocation and for discovering new drugs that block tumorigenesis by modifying the translocation of macromolecules.